ARTICLES
PUBLISHED ONLINE: 7 NOVEMBER 2016 | DOI: 10.1038/NPHYS3941
nature physics

Attosecond correlation dynamics

M. Ossiander[1,2*], F. Siegrist[1,2], V. Shirvanyan[1,2], R. Pazourek[3], A. Sommer[1], T. Latka[1,2], A. Guggenmos[1,4], S. Nagele[3], J. Feist[5], J. Burgdörfer[3], R. Kienberger[1,2] and M. Schultze[1,4*]

Photoemission of an electron is commonly treated as a one-particle phenomenon. With attosecond streaking spectroscopy we observe the breakdown of this single active-electron approximation by recording up to six attoseconds retardation of the dislodged photoelectron due to electronic correlations. We recorded the photon-energy-dependent emission timing of electrons, released from the helium ground state by an extreme-ultraviolet photon, either leaving the ion in its ground state or exciting it into a shake-up state. We identify an optical field-driven d.c. Stark shift of charge-asymmetric ionic states formed after the entangled photoemission as a key contribution to the observed correlation time shift. These findings enable a complete wavepacket reconstruction and are universal for all polarized initial and final states. Sub-attosecond agreement with quantum mechanical *ab initio* modelling allows us to determine the absolute zero of time in the photoelectric effect to a precision better than 1/25th of the atomic unit of time.

Photoemission of an electron occurs when the energy E_γ of the absorbed photon surpasses the ionization potential (IP) of the illuminated system. This hypothesis marks the foundation of quantum mechanics[1] and the process was tacitly regarded as an instantaneous single-particle phenomenon until the tools of attosecond time-resolved spectroscopy started to challenge these simplifications about a century after the photoelectric effect was postulated. When first experiments produced evidence for a delay in photoemission[2–6], it was recognized with recourse to a theoretical debate in the 1950s that the movement of the ionized electronic wavepacket through the attractive ionic potential can be interpreted as a (half-)scattering process leading to an energy-dependent phase shift as compared to its free movement in vacuum[7–9], which manifests as retardation or advance of the wavepacket[10–12]. In any multi-electron system, the correlated motion of the electrons arising from their mutual repulsion will cause dynamic modifications of the ionic potential which consequently affect the wavepacket's phase shift. The many-body problem of electronic correlations is a major communal challenge for chemistry[13], atomic, molecular and condensed matter physics[14]. Specifically in the latter field, a deepened understanding of these processes could cast light on many highly relevant phenomena that are mediated by electronic correlations—for example, electronic transport[15], phase transitions, magnetism[16] or superconductivity[17].

Precise experimental determination of the timing of photoemission can be a gateway to the investigation of electronic correlations. Since ionization delays have become an experimental observable they have posed a lively debated challenge for theory—see, for example, refs 18–26 and references therein. Even though both experimental methodology and theoretical treatment are still in their infancy, the first experimental observations could be explained qualitatively by a variety of theoretical approaches. The lack of quantitative agreement was attributed to the missing or incomplete description of electronic correlation in the theoretical approaches. Theory also indicated that a modification of the observed time shifts can arise from minute differences in the polarization of different states, which in turn can exert a back action on the outgoing electronic wavepacket[27–29].

An ideal test case for the experimental investigation of the role of electronic correlations is single photon (shake-up) ionization of helium, as sketched in Fig. 1. For the direct photoionization process, the outgoing photoelectron is promoted into the ionization continuum with kinetic energy $E_{\mathrm{kin}} = E_\gamma - \mathrm{IP}^{\mathrm{He}}$ (where the ionization energy of helium $\mathrm{IP}^{\mathrm{He}} = 24.6\,\mathrm{eV}$), leaving the remaining electron more strongly bound in the He^+ ground state (shake-down). Alternatively, for sufficiently energetic photons ($E_\gamma > 65.5\,\mathrm{eV}$) the electron remaining bound to the ion can be excited into one out of a series of ionic Rydberg states (shake-up (SU), or correlation satellites[30]) with excitation energies $\Delta E^{\mathrm{su}}_{n=2} = 40.8\,\mathrm{eV}$ (47.5, 50.2, 52.4, ... eV for $n = 3, 4, 5, \ldots$) converging towards the second ionization limit. The first process, also referred to as direct photoionization, can be described to a good degree of approximation within a single-particle framework, whereas the latter requires the interaction of both electrons and is a prototypical electronic correlation process. Such correlations evolve on the fast-paced attosecond timescale of electron dynamics and a measurement capable of resolving them would allow the isolation and exploration of the role of electronic correlations in the photoelectric effect and provide a benchmark for the refinement of high-level many-electron quantum theories.

Helium is the only multi-electron system for which the time-dependent Schrödinger equation including the quantum mechanical dynamics of all electrons in the presence of a laser field can be solved exactly[18]. For all heavier elements the inner electrons residing with the ion can be accounted for only approximately, for example, by density functional theories or Hartree–Fock methods[26]. Such approximate methods to describe electronic correlations limit the accuracy of the results obtained.

Earlier experimental studies of helium remained inconclusive due to the low photoabsorption cross-section at photon energies relevant for attosecond spectroscopy and low photon flux sources

[1]Max-Planck-Institut für Quantenoptik, Hans-Kopfermann-Strasse 1, 85748 Garching, Germany. [2]Physik-Department, Technische Universität München, James-Franck-Strasse 1, 85748 Garching, Germany. [3]Institute for Theoretical Physics, Vienna University of Technology, Wiedner Hauptstrasse 8-10, 1040 Vienna, Austria. [4]Fakultät für Physik, Ludwig-Maximilians-Universität München, Am Coulombwall 1, 85748 Garching, Germany. [5]Departamento de Física Teórica de la Materia Condensada and Condensed Matter Physics Center (IFIMAC), Universidad Autónoma de Madrid, 28049 Madrid, Spain.
*e-mail: marcus.ossiander@mpq.mpg.de; martin.schultze@mpq.mpg.de

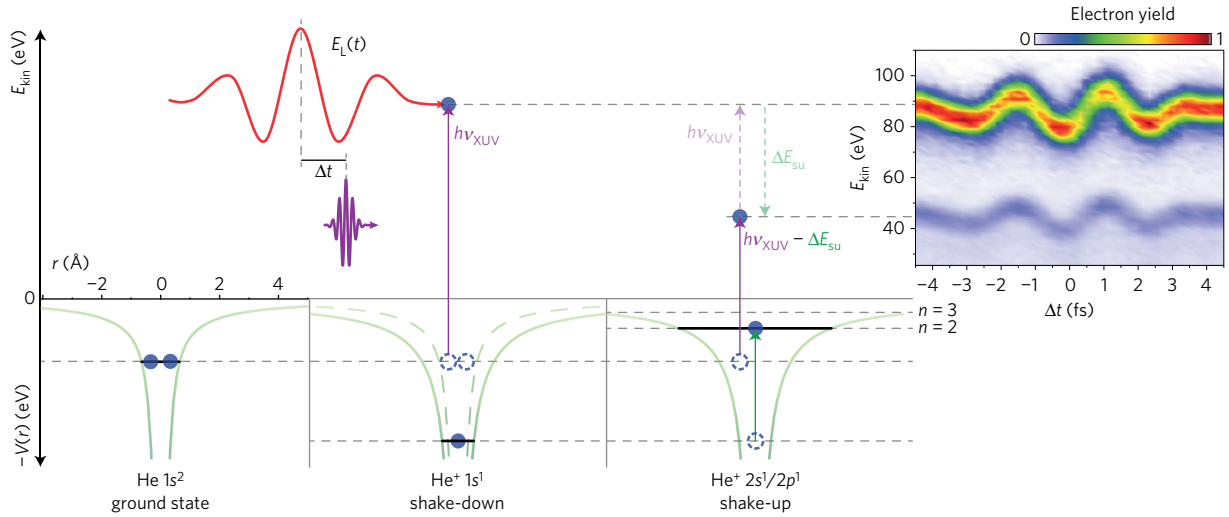

Figure 1 | Attosecond streaking spectroscopy of shake-up states in helium. Photoemission of an electron from the helium ground state (left panel) with a binding energy of 24.6 eV results in the liberation of the electron with a kinetic energy equal to the difference between photon energy and binding energy into the ionization continuum (middle panel). The ionic potential rearranges as result of the electron loss due to the modified screening of the nucleus, and the remaining electron occupies a more tightly bound state (shake-down or direct photoemission). Alternatively, the electron emission can be accompanied by the excitation of the remaining electron into one out of a series of shake-up states n (right panel). Due to electronic correlation, the escaping electron's kinetic energy is reduced by the excitation energy ΔE_{su}. In the presence of a time-delayed dressing laser field, the kinetic energy distribution of both quantum pathways is modulated according to the attosecond streak camera principle, permitting an accurate comparison of the electron release times. Electron yield is in arbitrary units.

resulting in large measurement uncertainties. Here we demonstrate how the advances of attosecond source technology now allow us to scrutinize the role of multi-electron interactions in the photoelectric effect. To our knowledge, this constitutes the first experimental study achieving both sub-attosecond precision and accuracy, evidenced by the near-perfect agreement with theory.

Observation of the relative photoemission timing

To explore the timing of helium photoelectrons we perform pump–probe experiments according to the attosecond streak camera scheme[31], where an isolated attosecond pump pulse liberates an electron in the presence of a laser electric probe field. The characteristic laser-induced modification of the photoelectron's kinetic energy depending on the arrival time difference between the two pulses can be used to track electronic processes with attosecond temporal resolution.

We synthesized attosecond pulses centred around photon energies of 93.9, 97.2, 108.2 and 112.8 eV (Fig. 2a) with a duration (full-width at half-maximum intensity) of 230, 180, 180, and 130 as, respectively, to investigate the photoemission timing and its energy dependence. Detection of the final electron momentum along the axis of laser polarization for different relative delay times between the attosecond pulse and the streaking laser field yields a spectrogram with contributions from both the direct photoionization and the shake-up channels, as shown in Fig. 1, right panel. We recorded ∼35 spectrograms for each central photon energy (representative raw data and details of the analysis methods can be found in the Supplementary Information). The data analysis is based on fitting a strong-field solution of the time-dependent Schrödinger equation to each spectrogram[2] with first-guess wavepackets for the reconstruction composed according to electron yield measurements performed at synchrotrons[30] convoluted with the attosecond pulse bandwidth (Fig. 2a). The semi-infinite dressing laser field integral, corresponding to the laser vector potential in the Coulomb gauge, $A(t) = -\int_{-\infty}^{t} E(t')\mathrm{d}t'$ is pre-determined from a first-moment fit to the individual electron spectra. The photon-energy dependence of the absorption cross-section and the small residual chirp of the attosecond pulses are accounted for in the data processing[32].

Attosecond streaking applied to helium is capable of recording the relative timing difference between direct and shake-up photoionization. The findings are summarized in Fig. 2b, where grey dots and error bars represent the experimental results for the relative timing difference between the ionization channels. The methodological refinements reported here allow the extraction of this quantity with unprecedented precision and yield an additional advance of the shake-up wavepacket of 12.6 ± 1.0 as at 93.9 eV photon energy (10.6 ± 0.9 as at 97.2 eV, 5.0 ± 1.0 as at 108.2 eV and 4.9 ± 1.6 as at 113.0 eV), as compared to photoemission without shake-up.

To contrast the experimental observations with fully correlated quantum mechanical modelling[33,34], we solve the time-dependent two-electron Schrödinger equation in its full dimensionality, including all inter-particle interactions. Our computational method is based on accurate state-of-the-art discretization and propagation schemes (see Supplementary Information), and has been successfully applied to various problems[18,34]. The computations are performed for central photon energies of 90, 95, 100, 110 and 120 eV, at a duration of 200 as (full-width at half-maximum intensity), and yield theoretical spectrograms that are analysed using the identical retrieval algorithm applied to extract timing information from the experimental data (black squares in Fig. 2b). Table 1 compares the theoretical and experimental results for the delay $\Delta\tau = \tau_{SU} - \tau_d$ between the release time τ_d of direct photoelectrons and the timing τ_{SU} of photoelectron emission accompanied by excitation of the shake-up manifold.

The remarkable agreement within the sub-attosecond standard error excludes systematic errors in the complex experiments and sophisticated numerical simulations.

With this confirmation, we can also employ the theoretical treatment to determine the absolute timing of photoemission from the relative measurement with sub-attosecond precision.

Absolute zero of time in the photoelectric effect

Since in the computations the arrival time of the attosecond pulse is known precisely, the energy-dependent absolute photoemission delay τ_d for direct photoionization can be determined accurately

Table 1 | Time shift $\Delta\tau$ between direct and shake-up photoemission in helium for different photon energies.

Photon energy (eV)	$\Delta\tau$ experiment (10^{-18} s)	Standard error (10^{-18} s)	$\Delta\tau$ theory (10^{-18} s)
93.9	−12.6	0.99	−12.7
97.2	−10.6	0.85	−11.0
108.2	−5.0	1.01	−5.9
113.0	−4.9	1.60	−5.8

from the numerically simulated spectrograms, which include electronic correlations to their full extent (black circles, Fig. 2b). We find absolute photoemission delays τ_d ranging from −4 to −6 as for the examined photon energies, corresponding to a temporal advance of the photoelectron wavepacket relative to the intensity maximum of the attosecond pulse. This time shift is accumulated by the outgoing wavepacket during its formation and propagation in the attractive ionic potential. The magnitude of the time shift corresponds to the Eisenbud–Wigner–Smith (EWS) delay τ_{EWS}, which describes the temporal behaviour of the (half-)scattering event in the ionic potential, and an additional modification τ_{CLC} (Coulomb-laser coupling) due to the long-range part of the ionic Coulomb potential which is dressed by the probing laser field[7,35]. Both contributions can be independently determined (see Supplementary Information) and the combined contribution yields the direct photoemission delay $\tau_d = \tau_{EWS} + \tau_{CLC}$. Such an alternative time-independent fully correlated quantum simulation based on the exterior complex scaling method[36] for the EWS delay plus CLC contribution (grey dashed line, Fig. 2b, for details see Supplementary Information) agrees to remarkable precision with the time shifts extracted from the simulated spectrograms. Furthermore, a single active-electron streaking simulation of the absolute time shift in direct photoemission using an effective potential based on the Hartree (mean-field) approximation (black dotted line, Fig. 2b) yields virtually identical results, highlighting the validity of a single-photon–single-electron description and the absence of significant electronic correlation effects for this ionization channel.

The absolute release time of the shake-up photoemission corresponds to the sum of τ_d and $\Delta\tau$ and can, in analogy to τ_d, be decomposed into different, independent contributions. In addition to the EWS and CLC time shifts, shake-up ionization is sensitive to an additional component due to the correlation between the emitted and the remaining electron in the presence of the probing infrared field.

Correlation-induced time shift

In contrast to neutral helium and the He^+ $1s^1$ ionic ground state, where the electrons are deeply bound and possess no dipole moment, and thus are insusceptible to the laser dressing field, the excited Rydberg states of the ion resulting from the shake-up transitions are strongly polarizable by the field due to their large spatial extent. The ionic eigenstates are assembled from a set of degenerate field-free sub-states of different orbital symmetries (for example, $2s$ and $2p$ for $n = 2$) which are energy-shifted in the laser electric field, resulting in the lifting of the degeneracy. The counterintuitive appearance of the d.c. Stark effect induced by the rapidly oscillating (a.c.) electric field of the laser with $(2\pi/\omega_{laser}) = 2.7$ fs period is a consequence of the temporal confinement of the photoelectron emission to the attosecond pulse duration. Since the dressing laser field amplitude is approximately constant during the temporal extent of the emanating electron wavepacket, the degeneracy of the field-free sub-states for each n is lifted by the instantaneous electric field.

Detection of the emitted electron in a particular direction breaks the inversion symmetry of the correlated two-electron system, as

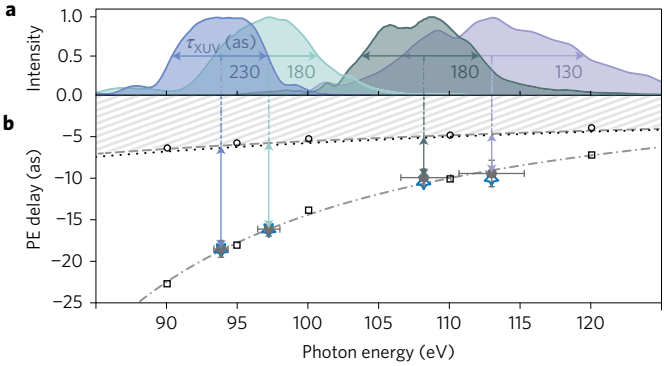

Figure 2 | Absolute timing of the photoelectric (PE) effect in helium. **a**, Spectral power of the attosecond pulses and durations (full-width at half-maximum intensity) extracted from the experiment. Intensity is in arbitrary units. **b**, The timing difference between the direct helium 1s and the shake-up electron emission is determined experimentally at central photon energies of 93.9, 97.2, 108.2 and 113 eV. Vertical arrows indicate the observed relative timing and vertical error bars denote the standard error of the mean determined from a set of measurements ($N \sim 35$, see Supplementary Information for histograms). Horizontal error bars indicate the maximum experimental uncertainty in the determination of the photon energy. Black circles depict the *ab initio* modelling results for the absolute photoemission delay of the shake-down process. The grey dashed line shows the result of a fully correlated but time-independent calculation and coincides with the predictions of a single active-electron model (black dotted line). *Ab initio* results for the shake-up ensemble photoemission delay are shown as black squares, together with an interpolation based on a single parameter fit following the universal energy dependence of the Coulomb-laser coupling and a constant offset (grey dash-dotted line). Blue stars represent full *ab initio* computations for exact experimental parameters (XUV pulse photon energy and bandwidth).

shown by the electron density distributions of the asymmetric ionic states $n = 2$ and $n = 3$ plotted in Fig. 3. As consequence of this asymmetry these states exhibit a finite, time-dependent dipole moment at the instant of photoemission.

The resulting effective dipole of the symmetry-broken singly charged ion exerts a back action on the outgoing electron, leading to a time shift of the emitted electron that is included in the fully correlated two-electron EWS delay. The additional presence of an (arbitrarily weak) probing laser field amends the total observed time shift τ_{su} for electrons leaving helium ions behind in a shake-up state by an additional contribution τ_{e-e} due to the correlation between the emitted and the remaining electron in the presence of the infrared field. Accordingly,

$$\tau_{su} = \tau_{EWS} + \tau_{CLC} + \tau_{e-e} \quad (1)$$

Whereas the streaking momentum shift follows the vector potential, the additional modification of the ionic energy levels due to the Stark effect follows the instantaneous dressing laser electric field. This quarter period phase lag results in an additional contribution to the photoemission delay governed by the effective dipole moment d_{eff} of the ion in the shake-up state and the initial momentum p_0 of the photoelectron[18]

$$\tau_{e-e} = \frac{1}{\omega_{laser}} \tan^{-1}\left(d_{eff}\frac{\omega_{laser}}{p_0}\right) \quad (2)$$

Since the vector potential and the electric field scale identically, the phase lag and the resulting correlation time τ_{e-e} are expected to be independent of the streaking laser field amplitude, as confirmed by our experiment within the operating range of attosecond streaking

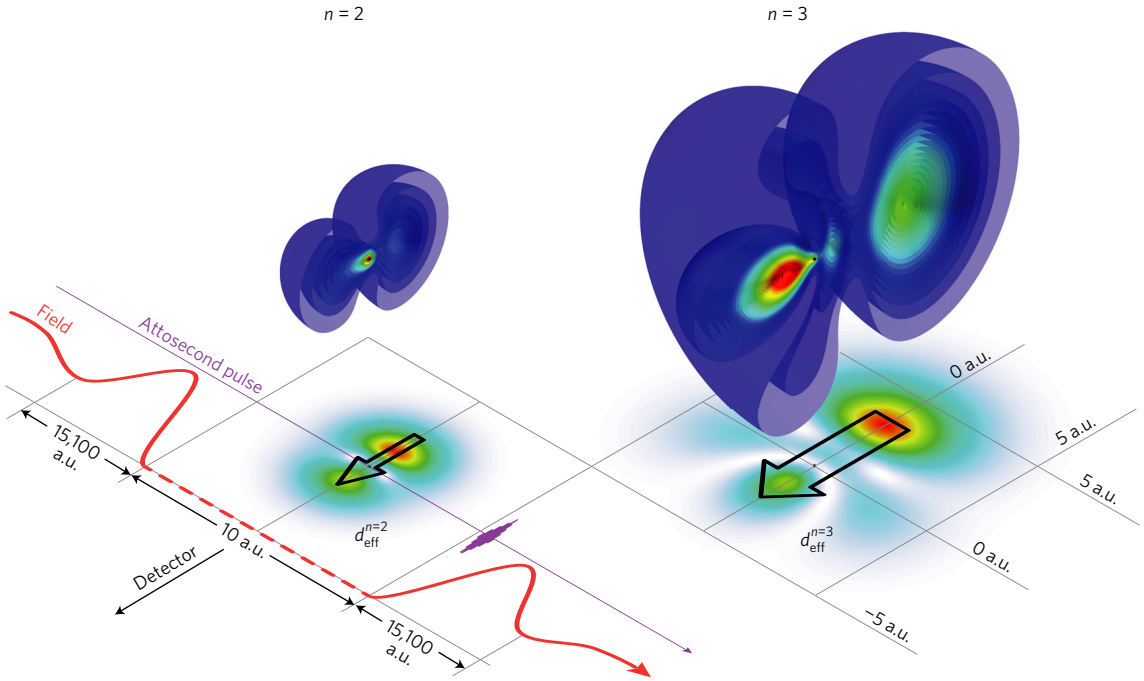

Figure 3 | The d.c. Stark effect at optical frequencies. False colour plot[43] of the electronic density distribution in the excited helium ionic $n=2$ and $n=3$ states after emission of a photoelectron. Discrimination of the detection direction (indicated by the arrow labelled 'Detector') results in an asymmetric charge density distribution carrying an effective dipole moment d_{eff} that couples to the laser electric field, which is approximately static in space and time for the duration of the attosecond pulse that triggers the photoemission.

($\sim$0.1–2 V Å^{-1}). By contrast, the induced dipole moment in the non-degenerate atomic/ionic ground state (a.c. Stark effect) scales quadratically with the laser electric field, and therefore does not cause a modification of the photoemission timing.

As a major advance of this work we can isolate the correlation time from the total observed time shift, since both τ_{EWS} and τ_{CLC} can be extracted from a rigorous time-independent calculation. Treating the experimental spectrograms with a frequency-resolved optical gating (FROG) analysis, the contribution of final states with principal quantum number $n>2$ can be suppressed (for details, see the Supplementary Information). For the isolated $n=2$ state the influence of electronic correlations on the observed time shift in the presence of the laser electric field is found to be as large as $\tau_{e-e}=6$ as, as shown in Fig. 4a. This correlation time exhibits a weaker dependence on the excitation photon energy than the total observed time shift, and manifests itself as an additional retardation of the outgoing wavepacket due to the multi-electron dynamics that is mediated by the spatially unbalanced charge density distribution of the ion after electron emission in the direction set by the detector. Since the correlation time is the time domain sequitur of the asymmetric ionic state polarization shown in Fig. 3, we can use τ_{e-e} to experimentally determine the effective dipole moment d_{eff} for the correlated shake-up wavepacket for the lowest principal quantum numbers. The results for a helium ion in the first excited state ($n=2$) are summarized in Fig. 4a. Since the charge density asymmetry of the excited ion plotted in Fig. 3 exhibits only a weak dependence on the excess energy of the outgoing photoelectron, the value for d_{eff} is expected to be almost independent of the excitation energy. We find a value of the dipole moment of $d_{\text{eff}}^{n=2}=0.32\pm 0.15$ a.u., in agreement within the error bars with the *ab initio* simulation, for which we get values of $d_{\text{eff}}^{n=2}\approx 0.42$. The observation of slightly lower values in the experiment is possibly rooted in the finite photoelectron acceptance angle, which includes wavepacket components into the detection that are emitted at a small angle with respect to the laser field polarization. Remarkably, $d_{\text{eff}}^{n=2}$ appears almost unaffected by the duration (that is, the spectral bandwidth) of the different attosecond pulses, which causes a varying degree of spectral overlap between consecutive shake-up states.

The additional contribution to the photoemission delay introduced in this work is not limited to the case of correlated emission accompanied by shake-up excitation, but is universal to any photoemission process that involves a polarized initial or final state or excites final states with a small energy difference. This includes photoemission from neon[2] or molecules that possess significantly higher dipole moments than helium.

Complete wavepacket reconstruction

Since both electrons are initially co-localized in the same atom, the outgoing photoelectron and the ion form a fully entangled quantum system. As a consequence of this entanglement, detection of the timing of the outgoing photoelectron thus reveals information about the evolving wavepacket and the dynamics of the residual ionic state in a non-destructive measurement.

The magnitude of $d_{\text{eff}}^{n=2}$ depends crucially on the occupation of the different $n=2$ sub-states $\Psi_{n=2}=c_{2s}\Psi_{2s}+c_{2p}\Psi_{2p}$. In turn, by extracting $d_{\text{eff}}^{n=2}$ from the precise timing recorded in an attosecond streaking experiment, information on the relative phase $\Delta\varphi$ between the amplitudes c_{2s} and c_{2p} of the wavepacket becomes accessible. The effective dipole moment depends on the relative transition probability $|c_{2s}/c_{2p}|^2$ into the different sub-states and their relative phase $\Delta\varphi$ according to

$$d_{\text{eff}}^{n=2}=2d_{+}^{n=2}\cos(\Delta\varphi)\frac{|c_{2s}/c_{2p}|}{1+|c_{2s}/c_{2p}|^2} \qquad (3)$$

where $d_{+}^{n=2}=3/2$ a.u. denotes the maximum dipole moment of an electron in the $n=2$ shell.

After the state superposition is prepared by the arrival of the attosecond pulse and photoelectron ejection, the ionic quantum state evolves in time. With the relative transition probabilities known from static experiments, the temporal dynamics of the ionic wavepacket can be determined, provided that phase difference $\Delta\varphi$

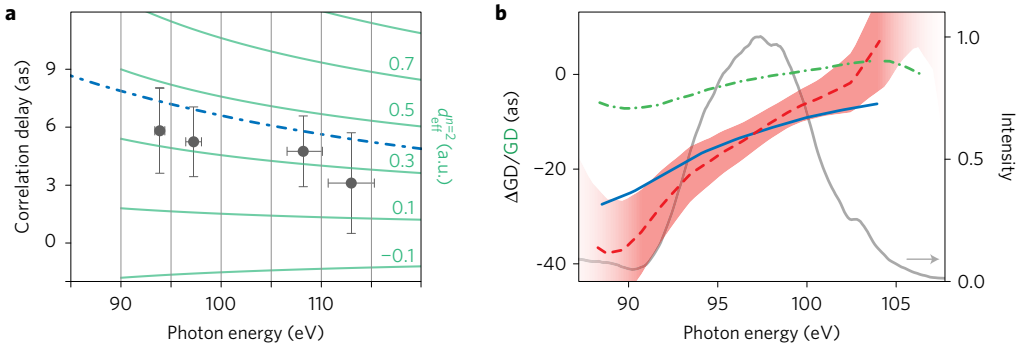

Figure 4 | Effective dipole moment for the $n=2$ shake-up state and relative group delay dispersion of the correlation time. a, Correlation delay τ_{e-e} as a function of the excitation photon energy and the derived effective dipole moment $d_{\mathrm{eff}}^{n=2}$ of the excited ionic state (right ordinate). Blue dash-dotted line: Theoretical prediction for $d_{\mathrm{eff}}^{n=2}$ based on *ab initio* modelling. Vertical error bars denote the standard error of the mean. Horizontal error bars indicate the maximum experimental uncertainty in the photon-energy determination. **b**, Frequency-resolved analysis of the recorded spectrograms within the bandwidth of the attosecond pulse (indicated by the grey line). Whereas the temporal phase of the direct helium 1s photoelectrons is almost constant across the attosecond pulse bandwidth (green dash-dotted line shows group delay), the shake-up photoelectron wavepacket exhibits a significant chirp that manifests as sweeping group delay difference (ΔGD). The red dashed line indicates ΔGD between the two channels computed from the experimental results (shaded area indicates the standard error of the mean) in comparison to the theoretical result (blue line). Within the bandwidth of the attosecond pulse (here centred at 97 eV) the measured group delay difference decreases as a function of the photon energy. Intensity is in arbitrary units.

is known. The attosecond streaking experiment yields the missing phase information. For the values of the correlation delay τ_{e-e} reported here and $c_{2s}/c_{2p} = 1.1 \pm 0.5$ at 97 eV (ref. 37), we find $\Delta\varphi = 1.35 \pm 0.17$ rad ($(c_{2s}/c_{2p})^{\mathrm{theory}} = 1.42$, $\Delta\varphi^{\mathrm{theory}} = 1.26$ rad), constant within the standard error for all investigated extreme-ultraviolet (XUV) photon energies (see Supplementary Information). The phase difference evaluated from the *ab initio* computations shows no dependence on the intensity of the applied laser electric field in the sampled range between 10^9 and 10^{12} W cm^{-2}. The experimental determination of $\Delta\varphi$ allows us to completely reconstruct the $n=2$ wavepacket (up to a global phase factor) and predict its time evolution after photoemission.

The attosecond XUV pulse with a spectral bandwidth (Fig. 2a) large compared to the energy difference of individual shake-up states excites multiple shake-up resonances simultaneously and launches a fully coherent electronic wavepacket that features rapid multi-state quantum beating. Furthermore, the presence of the laser field causes nontrivial coupling of higher shake-up channels. In this case, the unambiguous extraction of all relevant wavepacket phases is hindered. A spectrally narrow XUV pulse and a longer wavelength dressing field, however, permit the spectral isolation of the $n=3$ shake-up peak, as we show by a numerical streaking simulation in the Supplementary Information. In this setting, the correlation time τ_{e-e} is again found to be accurately predicted by $d_{\mathrm{eff}}^{n=3}$, although only partial reconstruction of the $n=3$ shake-up wavepacket can be achieved.

However, since the laser dressing of the photoelectron kinetic energy in the attosecond streak camera concept closely resembles frequency-resolved optical gating techniques[38] used to determine the temporal characteristics of ultrashort laser pulses, analysis of the experimental spectrograms can likewise determine the temporal and spectral phase characteristics of the emitted wavepackets[32]. This is of particular interest in the case of helium, where the comparison of the extracted spectral phase for the different ionization channels provides energy-resolved access to the role of multi-electron dynamics in the photoelectric effect that manifests itself in the reshaping of the outgoing photoelectron wavepacket. Figure 4b shows the group delay difference resulting from a FROG analysis of the recorded spectrograms at 97 eV excitation energy (details of the analysis and the adaptive algorithm are given in the Supplementary Information). Analogous analysis of the *ab initio* computations shows that the spectral phase of the electron wavepacket leaving the ion in its ground state coincides within the accuracy of our retrieval method to the phase evolution ('chirp') of the exciting attosecond pulse aside from a deviation due to Coulomb-laser coupling smaller than 0.15 as eV^{-1} and not exceeding 3 as over the whole energy range. The green dash-dotted line in Fig. 4b reveals a small residual chirp of the attosecond pulse becoming visible in the reconstructed group delay (GD) for the helium 1*s* photoemission. By using this signal as reference, we find that the wavepacket reconstructed for the shake-up process, by contrast, carries a significant spectral chirp which is associated to the variation of the quantum phase of the wavepacket in the correlated bound-free transition. Computing the difference between the two curves removes the small residual attosecond pulse chirp which affects both channels identically and yields a sweeping group delay difference ΔGD across the bandwidth of the excitation. The comparison to the group delay behaviour extracted from the *ab initio* spectrograms shows a remarkable agreement over the entire spectral range (Fig. 4b), highlighting the effectiveness of the *ab initio* computations to reproduce subtle multi-electron influences and the accuracy of the present experiment. Responsible for the temporal transformation of the debouching wavepacket are both the photon-energy dependence of the Coulomb-laser coupling and the electron correlation in the excitation process of the shake-up state.

Our work proves the validity of the non-relativistic two-electron time-dependent Schrödinger equation to an unprecedented level of accuracy of 10^{-19} s, and we have experimentally shown the complete characterization of the shake-up photoionization dynamics, providing a novel benchmark for the test and development of alternative multi-electron theories for more complex systems by spectrally resolved exploration of the group delay of the outgoing photoelectron wavepacket.

This first experimental study shedding light on the impact of electronic correlations on electron dynamics can serve as benchmark for the time-resolved exploration of their role in electronic transport and relaxation, magnetism and phase transitions, since attosecond spectroscopy has recently been successfully applied to study condensed matter systems[39–42]. In such experiments, helium can now serve as a tracer system for the determination of the absolute zero of time by adding it into a gas mixture or by simultaneous detection of photoelectron emission and transient XUV signatures from solid state systems. In a second step, such referential investigations will allow the replacement of helium by a referencing species that exhibits a significantly higher photoabsorption cross-section, or a binding energy best suited for the excitation wavelength, and

thus proliferate sub-attosecond absolute timing precision across ultrafast spectroscopy.

Methods

Methods, including statements of data availability and any associated accession codes and references, are available in the online version of this paper.

Received 3 June 2016; accepted 29 September 2016; published online 7 November 2016

References

1. Einstein, A. Über einen die Erzeugung und Verwandlung des Lichtes betreffenden heuristischen Gesichtspunkt. *Ann. Phys.* **322,** 132–148 (1905).
2. Schultze, M. *et al*. Delay in photoemission. *Science* **328,** 1658–1662 (2010).
3. Klünder, K. *et al*. Probing single-photon ionization on the attosecond time scale. *Phys. Rev. Lett.* **106,** 143002 (2011).
4. Eckle, P. *et al*. Attosecond ionization and tunneling delay time measurements in helium. *Science* **322,** 1525–1529 (2008).
5. Sabbar, M. *et al*. Resonance effects in photoemission time delays. *Phys. Rev. Lett.* **115,** 133001 (2015).
6. Palatchi, C. *et al*. Atomic delay in helium, neon, argon and krypton. *J. Phys. B* **47,** 245003 (2014).
7. Wigner, E. P. Lower limit for the energy derivative of the scattering phase shift. *Phys. Rev.* **98,** 145–147 (1955).
8. Eisenbud, L. *The Formal Properties of Nuclear Collisions* (Princeton Univ., 1948).
9. Smith, F. T. Lifetime matrix in collision theory. *Phys. Rev.* **118,** 349–356 (1960).
10. Nussenzveig, H. M. Time delay in quantum scattering. *Phys. Rev. D* **6,** 1534–1542 (1972).
11. de Carvalho, C. A. A. & Nussenzveig, H. M. Time delay. *Phys. Rep.* **364,** 83–174 (2002).
12. Sassoli de Bianchi, M. Time-delay of classical and quantum scattering processes: a conceptual overview and a general definition. *Centr. Eur. J. Phys.* **10,** 282–319 (2012).
13. Tew, D. P., Klopper, W. & Helgaker, T. Electron correlation: the many-body problem at the heart of chemistry. *J. Comput. Chem.* **28,** 1307–1320 (2007).
14. Fulde, P. *Electron Correlations in Molecules and Solids* (Springer Science & Business Media, 2012).
15. Datta, S. *Electronic Transport in Mesoscopic Systems* (Cambridge Univ. Press, 1997).
16. Auerbach, A. *Interacting Electrons and Quantum Magnetism* (Springer, 1994).
17. Hubbard, J. Electron correlations in narrow energy bands. *Proc. R. Soc. Lond. A* **276,** 238–257 (1963).
18. Pazourek, R., Feist, J., Nagele, S. & Burgdörfer, J. Attosecond streaking of correlated two-electron transitions in helium. *Phys. Rev. Lett.* **108,** 163001 (2012).
19. Dahlström, J. M., L'Huillier, A. & Maquet, A. Introduction to attosecond delays in photoionization. *J. Phys. B* **45,** 183001 (2012).
20. Nagele, S., Pazourek, R., Feist, J. & Burgdörfer, J. Time shifts in photoemission from a fully correlated two-electron model system. *Phys. Rev. A* **85,** 033401 (2012).
21. Kheifets, A. S. Time delay in valence-shell photoionization of noble-gas atoms. *Phys. Rev. A* **87,** 063404 (2013).
22. Zhang, C.-H. & Thumm, U. Streaking and Wigner time delays in photoemission from atoms and surfaces. *Phys. Rev. A* **84,** 033401 (2011).
23. Sukiasyan, S., Ishikawa, K. L. & Ivanov, M. Attosecond cascades and time delays in one-electron photoionization. *Phys. Rev. A* **86,** 033423 (2012).
24. Moore, L. R., Lysaght, M. A., Parker, J. S., van der Hart, H. W. & Taylor, K. T. Time delay between photoemission from the 2*p* and 2*s* subshells of neon. *Phys. Rev. A* **84,** 061404 (2011).
25. Baggesen, J. C. & Madsen, L. Atomic and molecular phases through attosecond streaking. *Phys. Rev. A* **83,** 021403(R) (2011).
26. Kheifets, A. S., Saha, S., Deshmukh, P. C., Keating, D. A. & Manson, S. T. Dipole phase and photoelectron group delay in inner-shell photoionization. *Phys. Rev. A* **92,** 063422 (2015).
27. Zhang, C.-H. & Thumm, U. Electron-ion interaction effects in attosecond time-resolved photoelectron spectra. *Phys. Rev. A* **82,** 043405 (2010).
28. Baggesen, J. C. & Madsen, L. B. Polarization effects in attosecond photoelectron spectroscopy. *Phys. Rev. Lett.* **104,** 043602 (2010).
29. Nagele, S. *et al*. Time-resolved photoemission by attosecond streaking: extraction of time information. *J. Phys. B* **44,** 081001 (2011).
30. Heimann, P. A. *et al*. Helium and neon photoelectron satellites at threshold. *Phys. Rev. A* **34,** 3782–3791 (1986).
31. Itatani, J. *et al*. Attosecond streak camera. *Phys. Rev. Lett.* **88,** 173903 (2002).
32. Yakovlev, V. S., Gagnon, J., Karpowicz, N. & Krausz, F. Attosecond streaking enables the measurement of quantum phase. *Phys. Rev. Lett.* **105,** 073001 (2010).
33. Feist, J. *et al*. Nonsequential two-photon double ionization of helium. *Phys. Rev. A* **77,** 043420 (2008).
34. Schneider, B. I. *et al*. *Quantum Dynamic Imaging* 149–208 (Springer Science & Business Media, 2011).
35. Ivanov, M. & Smirnova, O. How accurate is the attosecond streak camera? *Phys. Rev. Lett.* **107,** 213605 (2011).
36. Palacios, A., McCurdy, C. W. & Rescigno, T. N. Extracting amplitudes for single and double ionization from a time-dependent wave packet. *Phys. Rev. A* **76,** 043420 (2007).
37. Woodruff, P. R. & Samson, J. A. R. Measurements of partial cross sections and autoionization in the photoionization of helium to He^+ ($N=2$). *Phys. Rev. A* **25,** 848–856 (1982).
38. Trebino, R. *et al*. Measuring ultrashort laser pulses in the time-frequency domain using frequency-resolved optical gating. *Rev. Sci.* **68,** 3277–3295 (1997).
39. Vampa, G. & Villeneuve, D. M. High-harmonic generation: to the extreme. *Nat. Phys.* **11,** 529–530 (2015).
40. Luu, T. T. *et al*. Extreme ultraviolet high-harmonic spectroscopy of solids. *Nature* **521,** 498–502 (2015).
41. Ghimire, S. *et al*. Strong-field and attosecond physics in solids. *J. Phys. B* **47,** 204030 (2014).
42. Schultze, M. *et al*. Attosecond band-gap dynamics in silicon. *Science* **346,** 1348–1352 (2014).
43. Ramachandran, P. & Varoquaux, G. Mayavi: 3D visualization of scientific data. *Comput. Sci. Eng.* **13,** 40–51 (2011).

Acknowledgements

We acknowledge insightful comments and generous infrastructural support from F. Krausz. This work was supported by the Max Planck Society, the Deutsche Forschungsgemeinschaft Cluster of Excellence: Munich Centre for Advanced Photonics (http://www.munich-photonics.de), the Austrian Science Foundation project NEXTLITE (F049 and P23359-N16) and LASERLAB-EUROPE (grant agreement no. 654148, European Union's Horizon 2020 research and innovation programme). J.F. acknowledges funding by the European Research Council (ERC-2011-AdG Proposal 290981). R.K. acknowledges a Consolidator Grant from the European Research Council (ERC-2014-CoG AEDMOS). M.S. was supported by a Marie Curie International Outgoing Fellowship (FP7-PEOPLE-2011-IOF). The computational results presented have been achieved (in part) using the Vienna Scientific Cluster (VSC).

Author contributions

Experimental studies and analysis of experimental and theoretical signatures were carried out by M.O., F.S., V.S., A.S., T.L. and M.S. Theory and modelling were performed by R.P., supported by S.N. and J.F., and supervised by J.B. Customized XUV optics were provided by A.G. The manuscript was written by M.O., F.S. and M.S. All authors discussed the results and commented on the paper.

Additional information

Supplementary information is available in the online version of the paper. Reprints and permissions information is available online at www.nature.com/reprints. Correspondence and requests for materials should be addressed to M.O. or M.S.

Competing financial interests

The authors declare no competing financial interests.

Methods

We generate trains of extreme-ultraviolet (XUV) attosecond bursts by frequency upconversion of carrier-envelope-phase-stabilized, few-cycle, near-infrared laser pulses (1.2 mJ, 3.9 fs)[44] via high-order harmonic generation (HHG) in neon[45,46]. Isolated attosecond pulses are selected through spectral filtering of the XUV pulses achieved by the combination of dielectric or metallic bandpass mirrors and transmission through a thin metal foil[47]. The 150 nm molybdenum or palladium foil also compensates for the intrinsic frequency chirp of the high-harmonic radiation[48] in the cutoff region of the generated spectrum, allowing us to obtain near-Fourier-limited attosecond pulses.

A dispersion-free interferometric set-up allows us to raster scan the relative timing between the laser and attosecond pulses[49]. A grazing incidence toroidal mirror focusses both pulses collinearly onto an effusive jet of helium ($\rho \sim 10^{15}$ atoms cm^{-3}). The powerful laser source, optimized HHG parameters and the use of grazing incidence optics to transport the XUV radiation yields $>10^7$ photons (0.3 nJ) on target per attosecond pulse. This flux enables time-resolved spectroscopy even on samples with low absorption cross-section. The attosecond (pump) pulse ionizes a fraction of the helium atoms and the momentum of the released photoelectrons is measured by a time-of-flight spectrometer (for spectra and details of the energy conversion, see the Supplementary Information). Depending on the relative arrival time of the two pulses, the laser electric field (probe pulse) imparts a characteristic momentum shift on the outgoing photoelectron. To compensate for the difference in relative photoabsorption cross-section[50], an electrostatic einzel-lens assembly is used to selectively increase the electron spectrometer's energy-dependent acceptance angle.

Data availability. Raw data to validate alternative data analysis methods is available at the DOI: http://dx.doi.org/10.6084/m9.figshare.3859233. All data that support the plots within this paper and other findings of this study are available from the corresponding authors upon reasonable request.

References

44. Schweinberger, W. *et al*. Waveform-controlled near-single-cycle milli-joule laser pulses generate sub-10 nm extreme ultraviolet continua. *Opt. Lett.* **37,** 3573–3575 (2012).
45. Corkum, P. B. Plasma perspective on strong-field multiphoton ionization. *Phys. Rev. Lett.* **71,** 1994–1997 (1993).
46. Schafer, K. & Kulander, K. High harmonic generation from ultrafast pump lasers. *Phys. Rev. Lett.* **78,** 638–641 (1997).
47. Hofstetter, M. *et al*. Lanthanum–molybdenum multilayer mirrors for attosecond pulses between 80 and 130 eV. *New J. Phys.* **13,** 063038 (2011).
48. Mairesse, Y. *et al*. Attosecond synchronization of high-harmonic soft x-rays. *Science* **302,** 1540–1543 (2003).
49. Fiess, M. *et al*. Versatile apparatus for attosecond metrology and spectroscopy. *Rev. Sci.* **81,** 093103 (2010).
50. Becker, U. & Shirley, D. A. *VUV and Soft X-ray Photoionization* (Springer Science & Business Media, 2012).